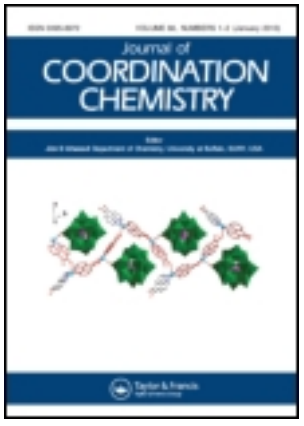

Journal of Coordination Chemistry
Publication details, including instructions for authors and subscription information:
http://www.tandfonline.com/loi/gcoo20

Studies on DNA binding behavior of biologically active Cu(II) complexes of Schiff bases containing acyl pyrazolones and 2-ethanolamine

Joseph V.A. [a b], Komal M. Vyas [a], Jignesh H. Pandya [b], Vivek K. Gupta [c] & R.N. Jadeja [a]

[a] Department of Chemistry, Faculty of Science, The M.S. University of Baroda, Vadodara, India

[b] Department of Chemistry, Christ College, Rajkot, India

[c] Post-Graduate Department of Physics, University of Jammu, Jammu Tawi, India

Accepted author version posted online: 14 Feb 2013.Published online: 21 Mar 2013.

To cite this article: Joseph V.A., Komal M. Vyas, Jignesh H. Pandya, Vivek K. Gupta & R.N. Jadeja (2013) Studies on DNA binding behavior of biologically active Cu(II) complexes of Schiff bases containing acyl pyrazolones and 2-ethanolamine, Journal of Coordination Chemistry, 66:6, 1094-1106, DOI: 10.1080/00958972.2013.776164

To link to this article: http://dx.doi.org/10.1080/00958972.2013.776164

Journal of Coordination Chemistry
Vol. 66, No. 6, 20 March 2013, 1094–1106

Studies on DNA binding behavior of biologically active Cu(II) complexes of Schiff bases containing acyl pyrazolones and 2-ethanolamine

JOSEPH V.A.†‡, KOMAL M. VYAS†, JIGNESH H. PANDYA‡, VIVEK K. GUPTA§ and R.N. JADEJA*†

†Department of Chemistry, Faculty of Science, The M.S. University of Baroda, Vadodara, India
‡Department of Chemistry, Christ College, Rajkot, India
§Post-Graduate Department of Physics, University of Jammu, Jammu Tawi, India

(*Received 14 April 2012; in final form 13 November 2012*)

Pyrazolone derivatives (*Z*)-4-((2-hydroxyethylimino)(*p*-tolyl)methyl)-3-methyl-1-phenyl-1*H*-pyrazol-5(4*H*)-one [PMP-EA] (**1**), (*Z*)-1-(3-chlorophenyl)-4-((2-hydroxyethylimino)(*p*-tolyl)methyl)-3-methyl-1*H*-pyrazol-5(4*H*)-one [MCPMP-EA] (**2**), and (*Z*)-4-((2-hydroxyethylimino)(*p*-tolyl)methyl)-3-methyl-1-*p*-tolyl-1*H*-pyrazol-5(4*H*)-one [PTPMP-EA] (**3**) have been synthesized and characterized. The molecular geometry of **2** has been determined by single-crystal X-ray study. These ligands exist in amine-one tautomeric form in the solid state. Three copper(II) complexes, [Cu(PMP-EA)$(H_2O)_2$] (**4**), [Cu(MCPMP-EA)$(H_2O)_2$] (**5**), and [Cu(PTPMP-EA)$(H_2O)_2$] (**6**), respectively, have been synthesized using these ligands and characterized by microanalytical data, molar conductivity, IR, UV–Visible, FAB-Mass, magnetic measurement, TG-DTA studies, and ESR spectral studies; Cu(II) is five-coordinated with [ML$(H_2O)_2$] composition. The interaction of the complexes with CT-DNA (calfthymus) was investigated using different methods. The results suggest that the copper complexes bind to DNA *via* intercalation and can quench the fluorescence intensity of EB bound to DNA.

Keywords: Schiff bases; Crystal structure; Cu(II) complexes; DNA binding

1. Introduction

Pyrazolone-5 derivatives form an important class of compounds important in medicinal chemistry for their high biological activity [1, 2]. Even the simplest pyrazolone-5 derivatives are well-known analgesics, widely used in medicine. 4-Acyl pyrazolone derivatives have many potential dimmers with diverse coordination, capable of chelating and bridging properties [3].

Schiff bases of acyl pyrazolones are ligands for many metal ions, promoted by high sensitivity with a series of ions. Schiff bases have diverse biological, pharmacological, antitumor activity and exceptional chelating ability [4–6].

*Corresponding author. Email: rajendra_jadeja@yahoo.com

Journal of Coordination Chemistry
ISSN 0095-8972 print/ISSN 1029-0389 online
http://dx.doi.org/10.1080/00958972.2013.776164

The chemistry of pyrazolone derivatives has expanded with synthesis of their metal complexes. Ligands and complexes possess strong biological activity [7]. Chemistry of pyrazolone containing metal complexes has been reviewed [8, 9].

Transition metal complexes have DNA binding affinity with open coordination positions for DNA binding and hydrolysis generating reactive oxygen containing species for DNA oxidation [10, 11]. We have opted for the biocompatible Cu(II), widely distributed in biological systems and its complexes have a broad spectrum of biological action. Cu accumulates in tumors due to selective permeability of the cancer cell membranes [12]. A number of copper complexes have been screened for anticancer activity both *in vivo* and *in vitro* [13]. Several Cu(II) Schiff base complexes have been the subject of investigation for DNA binding and cleavage [14–16]. Coordination compounds of copper, in both oxidation states, have been used in metal-mediated DNA cleavage through generation of hydrogen abstracting activated oxygen species [17, 18].

Our group has been actively engaged in studying 4-acyl pyrazolone derivatives and their complexes [19–24]. Among these studies, 4-acyl pyrazolone derivatives exhibit various coordination patterns and properties. However, little has appeared on the biological activity derived from 4-acylpyrazolone and 2-ethanolamine. Herein, we report the synthesis, structural characterization and biological activity of Cu(II) complexes.

In continuation to our previous work, dealing with the search for potent metal-based cancer chemotherapeutics, reduced toxicity and specific DNA target interaction [22, 23], we have carried out modulation of the Schiff base ligand scaffold.

2. Experimental

2.1. *Materials and methods*

Reagents and chemicals of analytical grade were procured from commercial sources. Solvents used for electrochemical and spectroscopic studies were purified using standard procedures [25]. The disodium salt of calf-thymus DNA (CT-DNA), purchased from Sigma, was stored at 4 °C and used as received. Stock solution of DNA was prepared by dissolving appropriate amount of DNA in H_2O and stored at 4 °C. The ratio of absorbance at 260 and 280 nm (A_{260}/A_{280}) was checked to be ~1.96, indicating that the DNA is sufficiently free from protein [26]. The concentration of DNA was determined spectrophotometrically at 260 nm after 1 : 100 dilution using the known molar extinction coefficient value of 6700 $M^{-1}\,cm^{-1}$ [27]. Ethidium bromide (EB) was obtained from Hi-media laboratories Pvt. Ltd., Mumbai. Double-distilled water was used for preparing all solutions. Purity of the ligands and complexes was evaluated by thin layer chromatography.

Elemental analyses (C, H, N) of the compounds were performed on a model 2400 Perkin–Elmer elemental analyzer. Infrared spectra (4000–400 cm^{-1}, KBr discs) of the samples were recorded on a model RX 1 FTIR Perkin-Elmer spectrophotometer. ^1H NMR spectra were recorded with a Bruker AV 400 MHz using DMSO-d_6 as solvent and TMS as an internal reference. The electronic spectra (in DMF at room temperature) from 400 to 800 nm were recorded on a Perkin-Elmer Lambda 35 UV–Vis spectrophotometer. GC–MS spectra of all the ligands were recorded on a Trace GC ultra DSQ II. Simultaneous TG/DTA was recorded on an EXSTAR6000 TG/DTA6300. Fluorescence spectra were recorded on a JASCO, FP-6300 fluorescence spectrophotometer. Molar conductivities of 10^{-3} M

solutions of the complexes in DMF were measured at room temperature with an Elico CM 180 direct reading digital conductivity meter. Copper was determined by EDTA after decomposing the complexes with HNO_3. Magnetic susceptibility measurements were carried out by employing the Guoy method at room temperature on a powdered sample of complexes using $[HgCo(CN)_4]$ as calibrant. ESR spectrum of the Cu(II) complex was recorded on a X-band instrument at the ESR laboratory, IIT, Bombay, at room temperature and liquid nitrogen temperature for polycrystalline and solution state, respectively.

2.2. *DNA binding experiments*

Absorption titration experiments for complexes were performed by maintaining constant metal complex concentration of 1 mM while varying the concentration of CT-DNA from 0 to 350 μM. From absorption data, the intrinsic binding constant K_b was determined from a plot of $[DNA]/(\varepsilon_a - \varepsilon_f)$ *versus* [DNA] using the equation:

$$[DNA]/(\varepsilon_a - \varepsilon_f) = [DNA]/(\varepsilon_b - \varepsilon_f) + [K_b(\varepsilon_b - \varepsilon_f)]^{-1}$$

where [DNA] is the concentration of DNA in base pairs. The apparent absorption coefficients ε_a, ε_f, and ε_b correspond to $A_{obsd}/[M]$ (where $M = Cu^{2+}$), to the extinction coefficient for free Cu(II) complex and to the extinction coefficient for the Cu(II) complex in the fully bound form, respectively.

Fluorescence quenching experiments were conducted by adding Cu(II) complex solution at different concentrations to the samples containing 3.3 μM EB and 3 μM DNA in buffer (150 mM NaCl and 15 mM trisodium citrate at pH 7.03). All the samples were excited at 546 nm and emission was recorded at 550–750 nm. The Stern–Volmer constant K_{sv} for each complex was calculated according to the following equation:

$$F_0/F = 1 + K_{sv}[Q]$$

where F_0 and F are the emission intensities in the absence and presence of quencher, respectively, Q is the concentration of the quencher and K_{sv} is the Stern–Volmer constant, obtained from the slope of the plot of F_0/F *versus* $[Q]$.

Viscosity experiments were carried out by using an Ostwald's capillary viscometer, immersed in a thermostated water bath with the temperature setting at 30 ± 0.1 °C for 15 min. DNA samples with an approximate average length of 200–500 base pairs were prepared by sonication in order to minimize complexities arising from DNA flexibility [4]. Flow time was measured with a digital stopwatch. Each sample was measured in triplicate and an average flow time was considered for the final calculation. Data were presented as $(\eta/\eta_0)^{1/3}$ *versus* the mole ratio of Cu(II) complex to DNA, where η is the viscosity of DNA in the presence of the complex and η_0 is the viscosity of DNA alone.

2.3. *Synthesis of PMP, MCPMP and PTPMP*

PMP (5-methyl-4-(4-methyl-benzoyl)-2-phenyl-2,4-dihydro-pyrazol-3-one), PTPMP (5-methyl-4-(4-methyl-benzoyl)-2-*p*-tolyl-2,4-dihydro-pyrazol-3-one), and MCPMP (2-(3-chloro-phenyl)-5-methyl-4-(4-methyl-benzoyl))-2,4-dihydro-pyrazol-3-one) were synthesized according to method reported [23].

2.4. *Synthesis of Schiff base ligands*

PMP (10 mmol) was dissolved in minimum absolute ethanol. To this solution, a solution of 2-ethanolamine (10 mmol) in 20 mL ethanol was added dropwise. The reaction mixture was refluxed for 6 h. After cooling a microcrystalline yellow compound separated, [PMP-EA] (**1**) was filtered, washed with water and then with ethanol and dried under vacuum.

A similar procedure was followed for synthesis of [MCPMP-EA] (**2**) and [PTPMP-EA] (**3**) using 2-(3-chloro-phenyl)-5-methyl-4-(4-methyl-benzoyl))-2,4-dihydro-pyrazol-3-one [MCPMP] and 5-methyl-4-(4-methyl-benzoyl)-2-*p*-tolyl-2,4-dihydro-pyrazol-3-one [PTPMP], respectively. Synthesis of the ligands is summarized by scheme 1.

1: Yield 81.85%, m.p. 150 °C. Anal. Calcd for $C_{20}H_{21}N_3O_2$ M.W.: 335.40, C(71.62%), H(6.31%), N(12.53%), found: C(71.28%), H(6.21%), N(12.91%); ^{1}H NMR (DMSO): δ 1.80(s, 3H, PZ C–CH_3), 3.19(s, 3H, TL C–CH_3), 7.02–7.41(m, 5H, Ph), 7.99–8.07(m, 4H, TL), 5.07(m, 1H, –OH), 3.42–3.45(t, 2H, N–CH_2–), 3.37–3.40(t, 3H, –CH_2–O), 11.23(s, 1H, –NH). IR (KBr, cm^{-1}): 3354(m) (O–H), 2924(m) (N–H), 1536(s) (C=N, cyclic), 1615 (m) (C=O, pyrazolone ring), 1222(s) (C=N, azomethane); MS: $m/z = 257.14$ $[C_{14}H_{16}N_3O_2]^+$, 97.08 $[C_4H_4N_2O]^+$.

2: Yield 82.68%, m.p. 165 °C. Anal. Calcd for $C_{20}H_{20}ClN_3O_2$ M.W.: 369.84, C (64.95%), H(5.45%), N(9.59%), found: C(64.41%), H(5.29%), N(9.66%); ^{1}H NMR (DMSO): δ 1.39(s, 3H, PZ C–CH_3), 3.20 (s, 3H, TL C–CH_3), 7.09–7.60(m, 4H, Ph), 7.96–8.05(m, 4H, TL), 5.08(s, 1H, –OH), 3.41–3.46(t, 2H, N–CH_2–), 3.49–3.52(t, 2H, –CH_2–O), 11.26(s, 1H, –NH). IR (KBr, cm^{-1}): 3418(m) (O–H), 2923(m) (N–H), 1539(s) (C=N, cyclic), 1620(m) (C=O, pyrazolone ring), 1227(s) (C=N, azomethane); MS: $m/z = 369.10$ $C_{20}H_{20}ClN_3O_2]^+$, 339.14 $[C_{18}H_{14}ClN_3O_2]^+$, 264.17 $[C_{12}H_{10}ClN_3O_2]^+$, 257.15 $[C_{14}H_{16}N_3O_2]^+$, 97.07 $[C_4H_4N_2O]^+$.

3: Yield 80.85%, m.p. 160 °C. Anal. calc. for $C_{21}H_{23}N_3O_2$ M.W.: 349.43, C(72.18%), H(6.63%), N(12.03%), found: C(72.68%), H(6.21%), N(12.51%); ^{1}H NMR (DMSO):

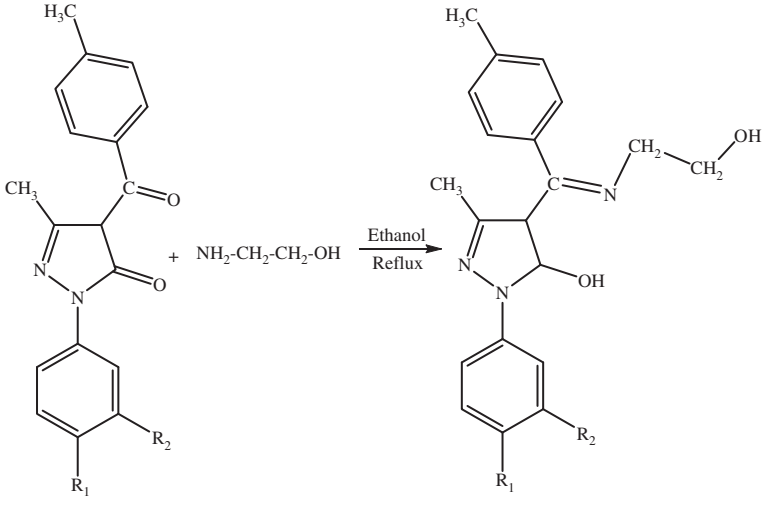

1: R_1=H, R_2=H; **2**: R_1=H, R_2=Cl; **3**: R_1=CH_3, R_2=H

Scheme 1. Synthesis of Schiff bases.

δ 1.34(s, 3H, PZ C–CH_3), 3.18 (s, 3H, TL C–CH_3), 7.07–7.39(m, 5H, Ph), 7.86–7.94(m, 4H, TL), 5.05(s, 1H, –OH), 3.44–3.45(t, 2H, N–CH_2–), 3.49–3.50(t, 2H, –CH_2–O), 11.24 (s, 1H, –NH). IR (KBr, cm^{-1}): 3347(m) (O–H), 2923(m) (N–H), 1526(s) (C=N, cyclic), 1607(m) (C=O, pyrazolone ring), 1220(s) (C=N, azomethane); MS: m/z = 349.28 $[C_{21}H_{23}N_3O_2]^+$, 348.10 $[C_{21}H_{22}N_3O_2]^+$, 200.03 $[C_{11}H_9N_2O_2]^+$, 119.13 $[C_8H_7O]^+$, 90.06 $[C_7H_7]^+$.

2.5. *Synthesis of Cu(II) complexes*

All the Cu(II) complexes of Schiff bases were prepared by the following method. Cu–acetate (2 mmol) was dissolved in a minimum amount of water and the solution was added to a hot ethanolic solution of the corresponding Schiff base (2 mmol). A crystalline solid formed, was filtered, washed with hot distilled water and then ethanol and dried under vacuum. Synthesis of the complexes is summarized by scheme 2.

[Cu(PMP-EA)(H_2O)$_2$] (**4**): Yield 58.62%, m.p.>250 °C. Anal. Calcd for $C_{20}H_{23}CuN_3O_4$: M.W.: 432.96, C(55.48%), H(5.35%), N(9.71%), Cu(14.68%), found: C (55.95%), H(5.76%), N(9.72%), Cu(14.81%). IR (KBr, cm^{-1}): 3429(m) (O–H coordinated H_2O), 1579(s) (C=N, cyclic), 1494(m) (C–O), 449(m) (Cu–N), 474(m) (Cu–O); MS: m/z = 431.2 $[C_{20}H_{22}CuN_3O_4]^+$, 370.3 $[C_{18}H_{17}CuN_3O_2]^+$, 372.3 $[C_{18}H_{19}CuN_3O_2]^+$, 327.2 $[C_{12}H_{15}CuN_3O_4]^+$, 235.1 $[C_7H_{14}CuN_3O_2]^+$, 202.3 $[C_{11}H_{11}N_3O]^+$, 122.0 $[C_5H_7N_3O]^+$. Electronic spectrum in DMF [λ/nm]: 638 ($d_{xz}, d_{yz} \rightarrow d_{x^2-y^2}$, square-pyramidal); Λ_M/S $m^2\,M^{-1}$ (in DMF, r.t.) = 39; μ_{eff} (B.M.) = 1.79.

[Cu(MCPMP-EA)(H_2O)$_2$] (**5**): Yield 59.86%, m.p.>260 °C. Anal. Calcd for $C_{20}H_{22}ClCuN_3O_4$: M.W.: 467.41, C(51.39%), H(4.74%), N(8.99%), Cu(13.60%), found: C (51.68%), H(4.67%), N(8.54%), Cu(13.51%). IR (KBr, cm^{-1}): 3430(m) (O–H coordinated H_2O), 1596(s) (C=N, cyclic), 1480(m) (C–O), 445(m) (Cu–N), 468(m) (Cu–O); MS:

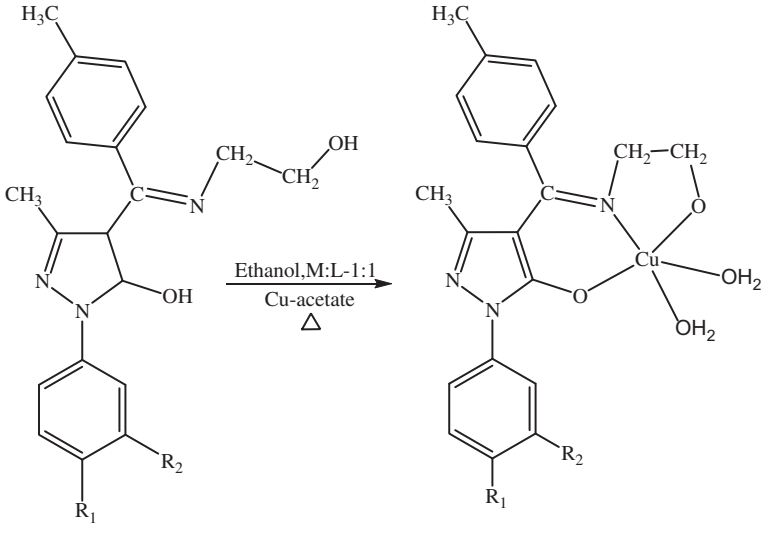

4: R_1=H, R_2=H; **5**: R_1=H, R_2=Cl; **6**: R_1=CH_3, R_2=H

Scheme 2. Synthesis of complexes.

m/z = 470.4 [M + 2 peak, $C_{20}H_{22}ClCuN_3O_4]^+$, 431 $[C_{20}H_{18}ClCuN_3O_2]^+$, 398.3 $[C_{20}H_{19}CuN_3O_2]^+$, 307.3 $[C_{13}H_{13}CuN_3O_2]^+$, 381.2 $[C_{19}H_{17}CuN_3O_2]^+$, 350.3 [base peak, $C_{18}H_{13}CuN_3O]^+$, 351.3 $[C_{18}H_{14}CuN_3O]^+$, 307.3 $[C_{18}H_{17}N_3O_2]^+$. Electronic spectrum in DMF [λ/nm]: 682 ($d_{xz}, d_{yz} \rightarrow d_{x^2-y^2}$, square-pyramidal); Λ_M/S m^2 M^{-1} (in DMF, r.t.) = 36; μ_{eff} (B.M.) = 1.76.

[Cu(PTPMP-EA)(H_2O)$_2$] (**6**): Yield 55.76%, m.p.>250 °C. Anal. Calcd for $C_{21}H_{25}CuN_3O_4$: M.W.: 446.99, C(56.43%), H(5.64%), N(9.40%), Cu(14.22%), found: C (56.75%), H(5.96%), N(9.72%), Cu(14.61%). IR (KBr, cm^{-1}): 3436(m) (O–H coordinated H_2O), 1597(s) (C=N, cyclic), 1477(m) (C–O), 430(m) (Cu–N), 478(m) (Cu–O); MS: *m/z* = 446.11 $[C_{21}H_{25}CuN_3O_4]^+$, 410.9 $[C_{21}H_{21}CuN_3O_2]^+$, 396 $[C_{20}H_{19}CuN_3O_2]^+$, 368 $[C_{18}H_{15}CuN_3O_2]^+$, 292 $[C_{12}H_{11}CuN_3O_2]^+$, 216 $[C_6H_7CuN_3O_2]^+$, 155 $[C_6H_9N_3O_2]^+$. Electronic spectrum in DMF [λ/nm]: 636 ($d_{xz}, d_{yz} \rightarrow d_{x^2-y^2}$, square-pyramidal); Λ_M/S m^2 M^{-1} (in DMF, r.t.) = 26; μ_{eff} (B.M.) = 1.78.

2.6. *X-ray structure determination*

Single-crystal X-ray diffraction for **2** was carried out. X-ray intensity data were collected on a Bruker CCD area-detector diffractometer equipped with graphite monochromated Mo Kα radiation (λ = 0.71073 Å) at 23 °C. The crystal used for data collection was of 0.30 × 0.20 × 0.20 mm. Cell dimensions were determined by least-square fit of angular settings of 5610 reflections in the θ range 2.48° < θ < 25.00°. The intensities were measured by $\varnothing$ and ω scan mode for θ range 3.42° to 25.00°. 2965 reflections were treated as observed ($I > 2\sigma(I)$). Data were corrected for Lorentz, polarization and absorption factors. The structure was solved by direct methods using SHELXS97 [28]. All nonhydrogen atoms of the molecule were located in the best E-map. Full-matrix least-squares refinement was carried out using SHELXL97 [28]. Atomic scattering factors were taken from International Tables for X-ray Crystallography (1992, Vol. C, tables 4.2.6.8 and 6.1.1.4). The crystallographic data are summarized in Supplementary material. An ORTEP [29] view of the ligand with atomic labeling is shown in Supplementary Material [30]. The geometry of the molecule has been calculated using the software PLATON [31] and PARST [32].

3. Results and discussion

The ligands were prepared by refluxing an appropriate amount of 4-toluoyl pyrazolone with 2-ethanolamine in ethanol. The structures of the synthesized ligands were established from IR, NMR and microanalytical data. Cu(II) complexes of these ligands were prepared by using the respective metal salt as acetate with the corresponding ligands in molar ratio of metal : ligand as 1 : 1.

The complexes are green, air and moisture-free amorphous solids, insoluble in common organic solvents but soluble in DMF and DMSO. Molar conductance values of the complexes in DMF (10^{-3} M solution at 25 °C) indicate that the complexes have molar ratio of metal:ligand as 1 : 1. The molar conductance values 39.00 (**4**), 36.00 (**5**), and 26.00 (**6**) Ohm^{-1} cm^2 mol^{-1} indicate that they are nonelectrolytes [33]. The magnetic moments of the complexes were recorded at room temperature for **4**, **5,** and **6** as 1.79, 1.76, and 1.78 BM, respectively, consistent with spin only value.

3.1. *Molecular structure of 2*

The molecular structure of **2** with the atom-numbering scheme is illustrated in Supplementary Material. The crystal packing of the ligand projected down the *a* axis is illustrated in Supplementary material. Important bond lengths and angles for the ligand are listed in Supplementary material. The crystal structure description is discussed in the Supplementary material.

3.2. *IR spectral studies*

The bonding mode of the ligand coordinated to Cu(II) ion was further elucidated by comparison with IR spectra of the ligands and complexes. From the crystal structure, we can see that the ligand exists as the keto form in the solid state. The broad peak at $\sim$2923 cm^{-1} in the free ligands corresponds to ν(N–H). Strong bands at $\sim$1536 and $\sim$1615 cm^{-1} are assigned to ν(C=N) and ν(C=O) of the pyrazolone ring, consistent with keto form in the solid state.

In IR spectra of the complexes, C=O and N–H stretches disappear and a new band attributed to ν(C–O) appears at $\sim$1480 cm^{-1}. Absorptions of C–OH and C=N slightly shift to lower wavenumber, indicating coordination of oxygen from 2-hydroxyethylimino and azomethane nitrogen. New bands at 445 and 468 cm^{-1} are assigned to Cu–N and Cu–O stretches. These results indicate that the ligand undergoes isomerization from keto to enol during coordination and then loses two protons to coordinate with Cu(II) as a double-negative bidentate ligand [34]. The IR spectra of **3** and its complex **6** are shown in Supplementary material.

3.3. *^{1}H NMR spectral studies*

The ^{1}H spectra of the ligands were carried out in DMSO-d_6 at room temperature. The data are reported along with possible assignments in the experimental section. All protons were found in their expected region. ^{1}H NMR spectrum of **1** is shown in Supplementary material.

3.4. *Electronic spectral studies*

Electronic spectra distinguish geometries of the complexes. Electronic absorption of the complexes in DMF solution shows a *d-d* transition at 550–660 nm, which can be assigned as the $d_{xz}, d_{yz} \rightarrow d_{x^2-y^2}$ transition, revealing that the Cu(II) is five-coordinated [35–39].

3.5. *Thermal studies*

Thermal stability and thermal behavior of the complexes were studied by thermogravimetric analysis (TGA–DTA–DTG) under nitrogen atmosphere from 25 to 700 °C. Correlations between decomposition steps of the complexes with the corresponding weight losses are almost the same for the complexes. No mass loss was observed up to 240 °C. The first decomposition at 250–310 °C probably is due to loss of coordinated water [40]. Above 300 °C, the complexes decompose gradually due to fragmentation and thermal degradation of the organic moiety; continuous loss of weight is observed up to 700 °C. This process is

accompanied by an exothermic process at 300 °C in DTA and DTG curves of the complexes. TG–DTA–DTG spectrum of **5** is given in Supplementary Material. For these complexes, mass loss corresponds to 8.31% (Calcd 8.35% for **4**), 7.24% (Calcd 7.20% for **5**), and 8.05% (Calcd 8.08% for **6**) for two water molecules. Thus, there are two coordinated waters in all three complexes.

3.6. *ESR spectral studies*

The X-band ESR spectra were recorded for solution and powder samples for **6** at RT and LNT (Supplementary material). The spectrum of the complex at 300 K shows one intense isotropic band in the high-field region. Hamiltonian parameters $g_{\|}$, $g_{\perp}$, $A_{\|}$, and $A_{\perp}$ were also calculated (table 1). For **6**, $G = 2.13$, indicating that the ligands are strong field ligands and the metal–ligand bonding in these complexes is covalent. It also indicates that the stereochemistry of the complex is square-pyramidal [41].

The orbital reduction factors ($K_{\|}$ and $K_{\perp}$) also indicate that the complex has covalent character and in-plane π-bonding is present in the complex. In the case of pure σ-bonding

Table 1. ESR parameters of **6**.

Hamiltonian parameters				Degree of geometrical distortion	Interaction coupling constant	Orbital reduction factors	
$g_{\|}$	$g_{\perp}$	$A_{\|}$	$A_{\perp}$	$g_{\|}/A_{\|}$	G	$K_{\|}$	$K_{\perp}$
2.21	2.10	260	20	85	2.13	0.794	0.0.418

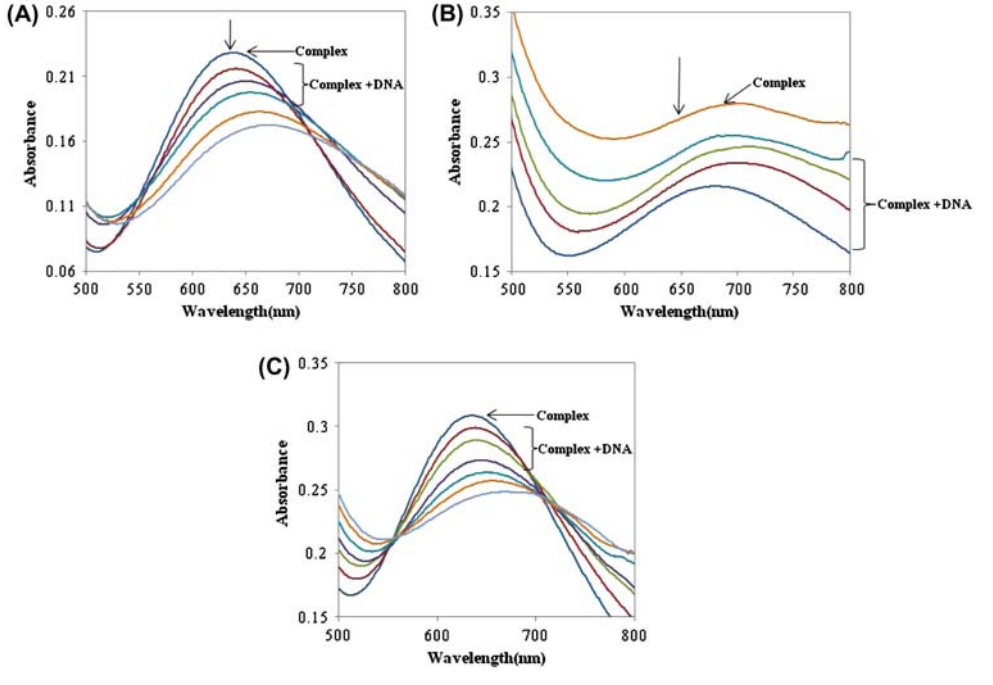

Figure 1. Electronic spectra of **4** (A), **5** (B) and **6** (C) (1×10^{-3} M) in DMF in the absence and presence of CT-DNA. The arrow shows the absorbance changes upon increasing DNA concentrations.

$K_{\|} = K_{\perp}$, whereas $K_{\|} < K_{\perp}$ implies considerable in-plane π-bonding, while for out-of-plane π-bonding $K_{\|} > K_{\perp}$. For the present complex, the observed order is $K_{\|}$ (0.79) > $K_{\perp}$ (0.41), implying a greater contribution from out-of-plane π-bonding than from in-plane π-bonding. In absence of any crystal structure evidence, from electronic and ESR spectral measurements, we predict square-pyramidal geometries for these five-coordinate copper complexes.

3.7. *Mass spectral studies*

Electron impact mass spectral data are reported in the experimental section. All the complexes give a molecular ion peak corresponding to their molecular weight. The GC–MS spectrum of **3** is shown in Supplementary material and representative ESI-mass spectra of **4** and **5** are shown in Supplementary material.

3.8. *DNA binding studies*

3.8.1. Absorption spectral studies. With increasing concentration of CT-DNA, absorptions of the complexes were affected, resulting in hypochromism and a slight red shift due to intercalative binding between DNA and the metal complexes. Hypochromism results from contraction of DNA in the helix axis, as well as from change in conformation, while hyperchromism results from damage of the DNA double helix structure [42–45].

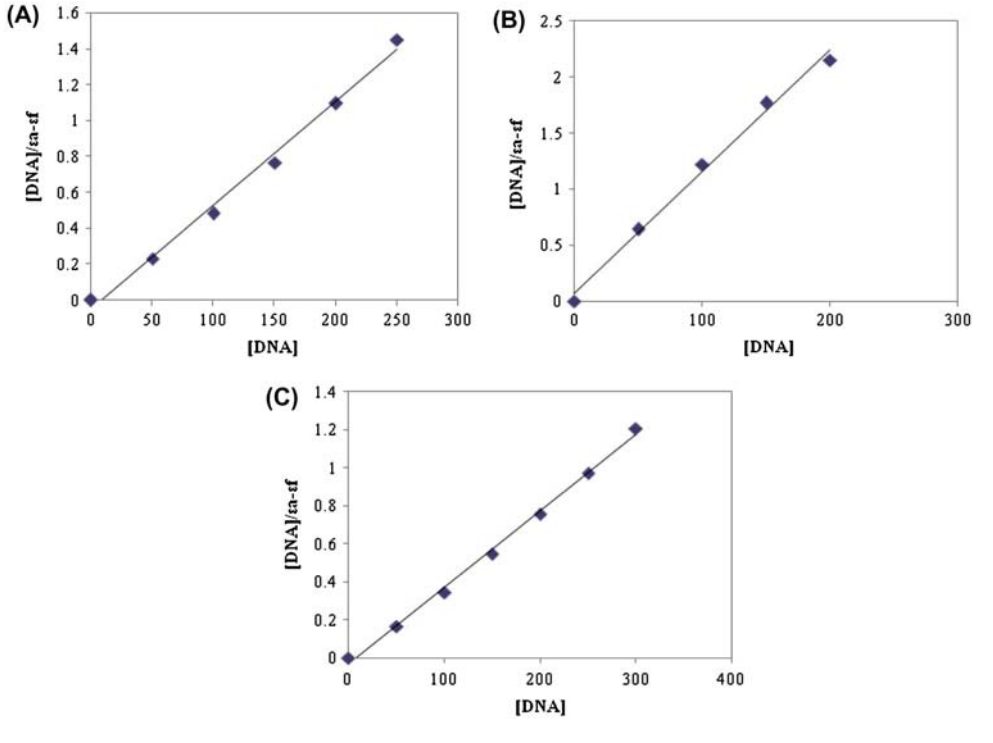

Figure 2. Plots of [DNA]/($\varepsilon_a - \varepsilon_f$) *vs.* [DNA] for titration of DNA with **4** (A), **5** (B) and **6** (C).

The absorption spectra of complexes in the absence and presence of DNA are given in figure 1.

To further illustrate the DNA binding strength, the intrinsic binding constant K_b was determined for the complexes as 0.9×10^5 M^{-1} (**4**), 1.2×10^5 M^{-1} (**5**), and 1.41×10^5 M^{-1} (**6**). The binding constants were lower than those observed for classical intercalators (ethidium-DNA, 1.4×10^6 M^{-1}) [46]. The diminution of the intrinsic binding constants could be explained by the steric constraints imposed by the ligand framework and thus encouraging a partial intercalation binding for the complexes. Our results are consistent with earlier reports on binding to DNA in Cu complexes [47, 48]. Plots of [DNA]/(ε_a–ε_f) *versus* [DNA] are shown in figure 2. From the values of the binding constants, **6** is strongest binder and the order of binding is **6** > **5** > **4**.

3.8.2. Competitive studies on DNA binding with EB. Further experiments were carried out to gain support for the mode of binding of the complexes with CT-DNA. Ethidium bromide was used which emits fluorescence in the presence of CT-DNA due to its strong intercalation. Quenching of the fluorescence of EB bound to DNA was measured with increasing amount of metal complexes.

As depicted in figure 3, the fluorescence intensity of EB decreases with increasing concentration of the complexes, indicating that some EB molecules are released from the EB–DNA complex after exchange with **4**, **5** and **6**. This may be due to either the metal

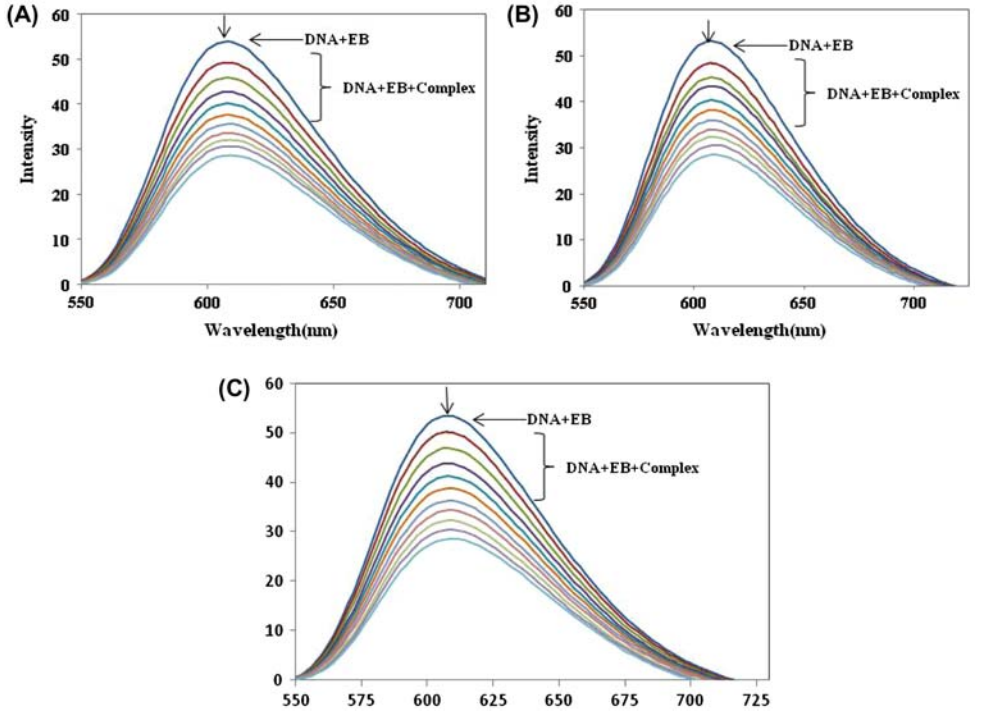

Figure 3. Emission spectra of EB bound to DNA in the absence and presence of **4** (A), **5** (B) and **6** (C). [EB] = 3.3 μM, [DNA] = 3 μM; λ_{ex} = 546 nm. The arrow shows intensity changes on increasing complex concentration.

complex competing with EB for DNA binding sites or a more direct quenching interaction on the DNA itself [46]. We assume the reduction in the emission intensity of EB on increasing the complex concentration could be caused by displacement of the DNA-bound EB by the Cu(II) complexes. Such quenched fluorescence of EB bound to DNA is also found in other copper complexes [49, 50]. A plot of relative fluorescence intensity (F_0/F) *versus* concentration for complexes is shown in figure 4.

Stern–Volmer constants calculated for all the complexes are 1.26×10^7 M^{-1}, $1.30 \times 10^7 M^{-1}$ and 1.31×10^7 M^{-1}, in agreement with literature [49, 50]. The values show that **6** has higher binding capacity than the other two complexes.

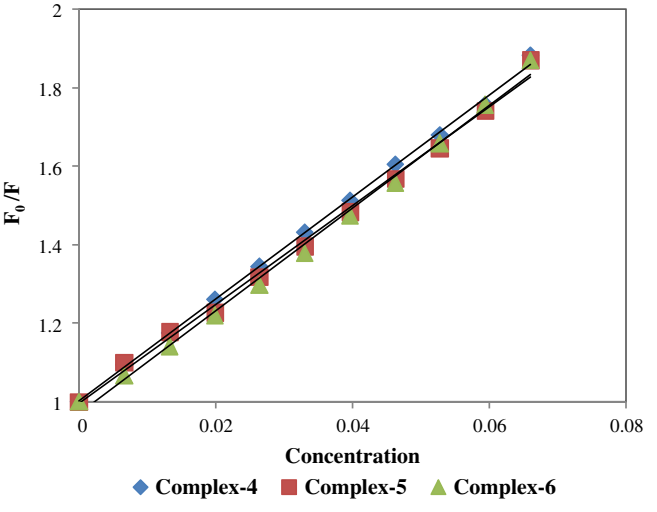

Figure 4. Plot of relative fluorescence intensity (F_0/F) *vs.* concentration for **4**–**6** in buffer solution (150 mM NaCl and 15 mM trisodium citrate at pH 7.03) ($\lambda_{em} = 610$ nm).

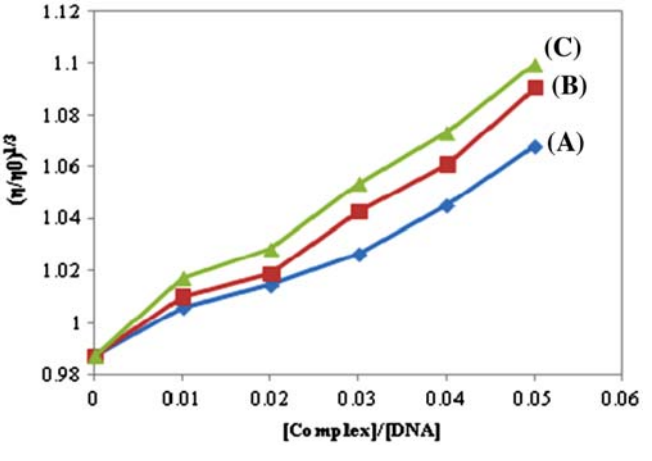

Figure 5. Effect of increasing amounts of **4** (A), **5** (B) and **6** (C) on the relative viscosities of DNA at 30.0 ± 0.1 °C. [DNA] = 50 μM, [Complex]/[DNA] = 0, 0.01, 0.02, 0.03, 0.04, 0.05, 0.06, respectively.

3.8.3. Viscosity studies. Binding of the complexes to CT-DNA was further investigated by viscometric studies. A classical intercalation results in lengthening of the DNA helix as the base pairs are separated to accommodate the binding molecule, leading to an increase in DNA viscosity. However, a partial and/or non-classical intercalation may bend (or kink) the DNA helix, resulting in decrease of its effective length and concomitantly its viscosity [45, 46, 51]. The effects of all the complexes on the viscosity of CT-DNA are shown in figure 5.

A significant increase in viscosity of DNA on addition of the complex due to intercalation increases the effective size of DNA, increasing the viscosity [52, 53]. The binding order of the complexes is **6** > **5** > **4**.

4. Conclusions

A series of Cu(II) complexes with Schiff base ligands derived from 4-toluoyl pyrazolones and 2-ethanolamine was synthesized and characterized. Spectral data show that all the Schiff bases are tridentate, bonding to Cu(II) through the deprotonated enol-O, deprotonated acidic-O, and azomethine nitrogen. Analytical data show the presence of one Cu(II) per one ligand and suggest a mononuclear square-pyramidal stereochemistry. The binding behavior of the metal complexes with DNA was studied by UV spectra, viscosity, and fluorescence assay under physiological conditions. All experimental evidence indicates that these complexes bind to CT-DNA *via* intercalation. Among the three complexes, **6** has highest binding affinity.

Supplementary material

CIF file for the X-ray crystal structure has been deposited with the Cambridge Crystallographic Data Center (CCDC 817981). Copies of this information can be obtained free of charge at www.ccdc.cam.ac.uk/conts/retrieval.html or from the CCDC, 12 Union Road, Cambridge CB2 1EZ, UK (Fax +44 1223/336 033. E-mail: deposit@ccdc.ac.uk).

Acknowledgements

The authors are thankful to the Head, Department of Chemistry, M.S. University of Baroda for providing necessary facilities required to carry out this work. The authors are also thankful to the management of the Christ College, Rajkot.

References

[1] R. Lesyk, O. Vladzimirska, V. Horishny, I. Nektegayev, I. Pshyk. *Sci. Pharm.*, **65**, 101 (1997).
[2] W.F. Yang, S.G. Yuan, Y.B. Xu, Y.H. Xiao, K.M. Fang. *J. Radioanal. Nucl. Chem.*, **256**, 149 (2003).
[3] G.C. Xu, L. Liu, L. Zhang, G.F. Liu, D.Z. Jia, J.P. Lang. *Struct. Chem.*, **16**, 431 (2005).
[4] D. Sinha, A.K. Tiwari, S. Singh, G. Shukla, P. Mishra, H. Chandra, A.K. Mishra. *Eur. J. Med. Chem.*, **43**, 160 (2008).
[5] M.S. Karthikeyan, D.J. Prasad, B. Poojary, K.S. Bhat, B.S. Holla, N.S. Kumari. *Bioorg. Med. Chem.*, **14**, 7482 (2006).
[6] S. Adsule, V. Barve, D. Chen, F. Ahmed, Q. Ping Dou, S. Padhye, F.H. Sarkar. *J. Med. Chem.*, **49**, 7242 (2006).

[7] C. Pettinari, F. Caruso, N. Zaffaroni, R. Villa, F. Marchetti, R. Pettinari, C. Phillips, J. Tanski, M. Rossi. *J. Inorg. Biochem.*, **100**, 58 (2006).
[8] F. Marchetti, C. Pettinari, R. Pettinari. *Coord. Chem. Rev.*, **249**, 2909 (2005).
[9] J.S. Casas, M.S. Garcıa-Tasende, A. Sanchez, J. Sordo, A. Touceda. *Coord. Chem. Rev.*, **251**, 1561 (2007).
[10] J. Tan, B. Wang, L. Zhu. *Bioorg. Med. Chem.*, **17**, 614 (2009).
[11] L.J.K. Boerner, J.M. Zaleski. *Curr. Opin. Chem. Biol.*, **9**, 135 (2005).
[12] D. Jayaraju, A.K. Kondapi. *Curr. Sci.*, **81**, 787 (2001).
[13] C. Marzano, M. Pellei, F. Tisato, C. Santini. *Med. Chem.*, **9**, 185 (2009).
[14] K. Dhara, P. Roy, J. Ratha, M. Manassero, P. Banerjee. *Polyhedron*, **26**, 4509 (2007).
[15] K. Dhara, J. Ratha, M. Manassero, X.-Y. Wang, S. Gao, P. Banerjee. *J. Inorg. Biochem.*, **101**, 95 (2007).
[16] V.C. da Silveira, J.S. Luz, C.C. Oliveira, I. Graziani, M.R. Ciriolo, A.M. da Costa Ferreira. *J. Inorg. Biochem.*, **102**, 1090 (2008).
[17] C. Tu, Y. Shao, N. Gan, Q. Xu, Z. Guo. *Inorg. Chem.*, **43**, 4761 (2004).
[18] B. Selvakumar, V. Rajendiran, P. Uma Maheswari, H.S. Evans, M. Palaniandavar. *J. Inorg. Biochem.*, **100**, 316 (2006).
[19] R.J. Yadav, K.M. Vyas, R.N. Jadeja. *J. Coord. Chem.*, **63**, 1820 (2010).
[20] K.M. Vyas, V.K. Shah, R.N. Jadeja. *J. Coord. Chem.*, **64**, 1069 (2011).
[21] K.M. Vyas, R.N. Jadeja, V.K. Gupta, K.R. Surati. *J. Mol. Struct.*, **990**, 110 (2011).
[22] K.M. Vyas, R.G. Joshi, R.N. Jadeja, C. Ratna Prabha, V.K. Gupta. *Spectrochim. Acta, Part A*, **84**, 256 (2011).
[23] R.N. Jadeja, K.M. Vyas, V.K. Gupta, R.G. Joshi, C. Ratna Prabha. *Polyhedron*, **31**, 767 (2012).
[24] S. Parihar, S. Pathan, R.N. Jadeja, A. Patel, V.K. Gupta. *Inorg. Chem.*, **51**, 1152 (2012).
[25] W.L.F. Armarego, D.D. Perrin. *Purification of Laboratory Chemicals*, 4th Edn, The Bath Press/–Butterworth-Heinemann Publication, Oxford (1997).
[26] J. Marmur. *J. Mol. Biol.*, **211**, 3208 (1961).
[27] M.E. Reichman, S.A. Rice, C.A. Thomas, P. Doty. *J. Am. Chem. Soc.*, **76**, 3047 (1954).
[28] G.M. Sheldrick. *SHELX97*, University of Gottingen, Germany (1997).
[29] C.K. Johnson. *ORTEP II; Report ORNL-5138*, Oak Ridge National Laboratory, Oak Ridge, TN (1976).
[30] L.J. Farrugia. *J. Appl. Cryst.*, **30**, 565 (1997).
[31] A.L. Spek, *PLATON for Windows*. September 1999 Version, University of Utrecht, The Netherlands (1999).
[32] M. Nardelli. *J. Appl. Cryst.*, **28**, 659 (1995).
[33] W.J. Geary. *Coord. Chem. Rev.*, **7**, 81 (1971).
[34] B.T. Thaker, K.R. Surati, S. Oswal, R.N. Jadeja, V.K. Gupta. *Struct. Chem.*, **18**, 295 (2007).
[35] A.B.P. Lever. *Inorganic Electronic Spectroscopy*, 2nd Edn Edn, Elsevier, Amsterdam (1984).
[36] F.A. Mautner, C.N. Landry, A.A. Gallo, S.S. Massoud. *J. Mol. Struct.*, **837**, 72 (2007).
[37] B.J. Hathaway. *J. Chem. Soc., Dalton Trans.*, **1**, 1196 (1972).
[38] B.J. Hathaway. In: G. Wilkinson, R.D. Gillard, J.A. McCleverty (Eds.), *Comprehensive Coordination Chemistry*, Vol. 5, p. 533, Pergamon Press, Oxford, UK (1987).
[39] U. Mukhopadhyay, I. Bernal, S.S. Massoud, F.A. Mautner. *Inorg. Chim. Acta*, **357**, 3673 (2004).
[40] C.K. Modi, M.N. Patel. *J. Therm. Anal. Calorim.*, **94**, 247 (2008).
[41] P. Uma Maheswari, M. Palaniandavar. *Inorg. Chim. Acta*, **357**, 901 (2004).
[42] A. Colak, U. Terzi, M. Col, S.A. Karaoglu, S. Karabocek, A. Kucukdumlu, F.A. Ayaz. *Eur. J. Med. Chem.*, **45**, 5169 (2010).
[43] S.-H. Cui, M. Jiang, Y.-T. Li, Z.-Y. Wu. *X-W. Li. J. Coord. Chem.*, **64**, 4209 (2011).
[44] N. Raman, K. Pothiraj, T. Baskaran. *J. Coord. Chem.*, **64**, 4286 (2011).
[45] Y. Mei, J.-J. Zhou, H. Zhou, Z.-Q. Pan. *J. Coord. Chem.*, **65**, 643 (2012).
[46] J.B. Le Pecq, C. Paoletti. *J. Mol. Biol.*, **27**, 87 (1967).
[47] F. Arjmand, M. Aziz. *Eur. J. Med. Chem.*, **44**, 834 (2009).
[48] N. Raman, R. Jeyamurugan, A. Sakthivel, L. Mitu. *Spectrochim. Acta, Part A*, **75**, 88 (2010).
[49] U. McDonnell, M.R. Hicks, M.J. Hannon, A. Rodger. *J. Inorg. Biochem.*, **102**, 2052 (2008).
[50] M. Shakir, S. Khanam, M. Azam, M. Aatif, F. Firdaus. *J. Coord. Chem.*, **64**, 3158 (2011).
[51] S. Sathyanarayana, J.C. Dabroniak, J.B. Chaires. *Biochemistry*, **31**, 9319 (1992).
[52] S. Satyanarayana, J.C. Dabrowiak, J.B. Chaires. *Biochemistry*, **32**, 2573 (1993).
[53] N. Raman, K. Pothiraj, T. Baskaran. *J. Coord. Chem.*, **64**, 3900 (2011).